

# PRL1 modulates root stem cell niche activity and meristem size through *WOX5* and *PLTs* in *Arabidopsis*

Hongtao Ji<sup>1</sup>, Shuangfeng Wang<sup>1,2</sup>, Kexue Li<sup>1</sup>, Dóra Szakonyi<sup>3,†</sup>, Csaba Koncz<sup>3,4</sup> and Xia Li<sup>1,\*</sup>

<sup>1</sup>The State Key Laboratory of Plant Cell and Chromosome Engineering, Center for Agricultural Research Resources, Institute of Genetics and Developmental Biology, Chinese Academy of Sciences, 286 Huaizhong Road, Shijiazhuang, Hebei 050021 China,

<sup>2</sup>University of Chinese Academy of Sciences, No.19A Yuquan Road, Beijing 100049 China,

<sup>3</sup>Max-Planck Institute for Plant Breeding Research, Carl-von-Linné-Weg 10, Cologne, D-50829 Germany, and

<sup>4</sup>Institute of Plant Biology, Biological Research Center of Hungarian Academy of Sciences, Temesvári krt. 62, Szeged H-6726 Hungary

Received 7 November 2014; revised 20 November 2014; accepted 21 November 2014; published online 29 November 2014.

\*For correspondence (e-mail xli@genetics.ac.cn).

†Present address: Plant Molecular Biology, Instituto Gulbenkian de Ciência, Oeiras, Portugal.

## SUMMARY

The stem cell niche in the root meristem maintains pluripotent stem cells to ensure a constant supply of cells for root growth. Despite extensive progress, the molecular mechanisms through which root stem cell fates and stem cell niche activity are determined remain largely unknown. In *Arabidopsis thaliana*, the *Pleiotropic Regulatory Locus 1 (PRL1)* encodes a WD40-repeat protein subunit of the spliceosome-activating Nineteen Complex (NTC) that plays a role in multiple stress, hormone and developmental signaling pathways. Here, we show that PRL1 is involved in the control of root meristem size and root stem cell niche activity. PRL1 is strongly expressed in the root meristem and its loss of function mutation results in disorganization of the quiescent center (QC), premature stem cell differentiation, aberrant cell division, and reduced root meristem size. Our genetic studies indicate that PRL1 is required for confined expression of the homeodomain transcription factor *WOX5* in the QC and acts upstream of the transcription factor *PLETHORA (PLT)* in modulating stem cell niche activity and root meristem size. These findings define a role for PRL1 as an important determinant of PLT signaling that modulates maintenance of the stem cell niche and root meristem size.

**Keywords:** *Arabidopsis thaliana*, PRL1, root stem cell niche, root meristem, *WOX5*, *PLT*.

## INTRODUCTION

In higher plants, root growth is maintained by coordinating cell proliferation and differentiation. *Arabidopsis thaliana* is a model plant with typical allorhiz roots consisting of three concentric layers (epidermis, cortex, and endodermis) surrounding the stele, which contains the vascular tissues (Dolan *et al.*, 1993). Root tissue cells are derived from the stem cell niche, comprised of an inner group of mitotically inactive quiescent center (QC) cells and outer mitotically active stem cells (van den Berg *et al.*, 1995; Scheres, 2007; Dinneny and Benfey, 2008). The stem daughter cells divide several times in the proximal meristem, and then differentiate in the transition zone (Ubeda-Tomas and Bennett, 2010). Thus, root meristem size is maintained by the balance between cell division and differentiation in the root meristematic zone.

In recent decades, an extensive effort has been mounted to understand the molecular mechanism by which the function of QC and activity of stem cell niche is controlled in *Arabidopsis* roots. Several key regulators of QC identity and stem cell niche activity were identified (Di Laurenzio *et al.*, 1996; Aida *et al.*, 2004; Sarkar *et al.*, 2007). One of these, the WUSCHEL-RELATED HOMEBOX5 (*WOX5*) factor, is specifically expressed in the QC and functions as a chief regulator of QC maintenance and tissue homeostasis in the root meristem. Loss of *WOX5* function was demonstrated to cause terminal differentiation of distal root stem cells (Sarkar *et al.*, 2007). Other genes controlling the maintenance of QC identity and root stem cell niche activity include *SHORT-ROOT (SHR)* and *SCARECROW (SCR)* that code for putative GRAS transcription factors. SHR is mainly

expressed in the stele and can move to the QC and other surrounding cells to activate *SCR* expression together with *WOX5* for coordinate regulation of QC identity and the balance between root stem cell division and differentiation. Mutations of *SHR* and *SCR* result in aberrant stem cell niche morphology and defective root meristem (Di Laurenzio *et al.*, 1996; Helariutta *et al.*, 2000; Sabatini *et al.*, 2003) indicating that the *SHR/SCR* pathway regulates QC identity and stem cell niche activity.

In parallel with the *SHR/SCR* pathway, QC maintenance and root meristem homeostasis are controlled by the *PLETHORA (PLT)* family of AP2-domain transcription factors. *PLT1* and *PLT2* are required for maintenance of the activity and determine the position of stem cell niche (Aida *et al.*, 2004; Galinha *et al.*, 2007). *PLT1* and *PLT2* mediate positioning of the QC depending on local auxin maximum and regulate stem cell niche activity responding to the auxin gradient (Blilou *et al.*, 2005; Grieneisen *et al.*, 2007; Dinneny and Benfey, 2008). Both *PLT1* and *PLT2* are induced by auxin and exhibit a graded expression in the root meristem reflecting the distribution of auxin (Aida *et al.*, 2004; Galinha *et al.*, 2007; Grieneisen *et al.*, 2007). The *PIN* auxin efflux carriers play a key role in controlling *PLT1/PLT2* expression in the distal root meristem (Blilou *et al.*, 2005; Ding and Friml, 2010). In turn, *PLT1/PLT2* regulate root-specific *PIN* expression and polar localization of PINs (Blilou *et al.*, 2005; Galinha *et al.*, 2007; Pinon *et al.*, 2013). Thus, a feedback loop between auxin homeostasis and *PLT1/PLT2* expression controls root meristem maintenance. Recently, it has been shown that the RAC/ROP GTPase activator RopGEF7, which is expressed in an auxin-dependent manner, is involved in transmission of the auxin signal to *PLT1/PLT2* in the QC (Chen *et al.*, 2011a). Other data indicate that *WOX5* acts upstream of the *PLT1* to regulate auxin-mediated QC determination and root stem cell niche homeostasis (Ding and Friml, 2010). Maintenance of quiescence in the QC and root stem cell activity is a complex process, which also modulated by abscisic acid (ABA), ethylene, jasmonate, and brassinosteroids, and several metabolic and stress signaling pathways (Zhang *et al.*, 2010; Chen *et al.*, 2011b; Hacham *et al.*, 2011; Takatsuka and Umeda, 2014). Nonetheless, many important modules that link hormone signaling to the cell cycle machinery and maintenance of root stem cell niche are unknown.

Here, we report on the identification of a *meristem changed root 1 (mcr1)* mutation, which reduces root meristem size and stem cell niche activity. The *mcr1* mutation proved to be allelic with the *prl1* mutation, which inactivates the *Pleiotropic Regulatory Locus 1 (PRL1)* that codes for a conserved WD40-repeat protein subunit of the nuclear spliceosome-activating Nineteen Complex (NTC) (Koncz *et al.*, 2012). *PRL1* was originally identified as an important pleiotropic regulator of plant responses to sugars, multiple

hormones including auxin, ABA, cytokinin, and ethylene; cold stress and defense responses to bacterial and fungal pathogens (Németh *et al.*, 1998; Palma *et al.*, 2007). The *prl1* mutation results in transcriptional derepression of glucose-responsive genes, whereas the *PRL1* protein interacts with the Arabidopsis sucrose non-fermenting 1 (SNF1) homologs AKIN10 and AKIN11 (Bhalerao *et al.*, 1999), which are central regulators of cellular energy homeostasis and signaling (Baena-González *et al.*, 2007). *PRL1* was reported to function as substrate receptor of CUL4–ROC1–DDB1–*PRL1* (CULLIN4–REGULATORS OF CULLINS–DAMAGED DNA BINDING 1) E3 ubiquitin ligase involved in the degradation of AKIN10 (Lee *et al.*, 2008).

All *prl1* mutant alleles, including *mcr1* cause dramatic defects in root development (Németh *et al.*, 1998; Palma *et al.*, 2007). By studying the underlying mechanism, here we show that *PRL1* functions upstream of *PLT1/PLT2* to modulate stem cell niche activity and root meristem size in Arabidopsis. *PRL1* modulates root stem cell niche activity and root apical meristem (RAM) size by maintaining graded expression of *PLT1/PLT2* and expression of the downstream effector *WOX5* in the QC. Furthermore, *PRL1* is required for maintenance of columella stem cell (CSC) and provascular stem cell (PSC) activities. Collectively, these results show that *PRL1* is necessary for QC maintenance, stem cell niche activity, root meristem size, and induction of *PLT1/PLT2* and *WOX5* in Arabidopsis roots.

## RESULTS

### Isolation of a mutant defective in root meristem size and cell differentiation

To identify novel determinants involved in the control of root meristem activity, a genetic screen using 3000 independent T-DNA mutagenized lines (Zuo *et al.*, 2000) was performed by monitoring with root length and elongation. One short root mutant showing an altered apical root meristem was named *mcr1*. As illustrated in Figure 1(a), the *mcr1* mutant showed a short root phenotype when grown on Murashige and Skoog (MS) medium. The primary root length and size of the meristem of *mcr1* seedlings were substantially reduced (Figure 1(b–d)). The number of cells in the meristem, defined as the number of cortical cells in a file extending from the initial cell adjacent to the QC to the first elongated cell (Dello Iorio *et al.*, 2007), was obviously decreased in the *mcr1* mutant compared with wild type (Figure 1(c, d)). The number of evenly sized cortical cells in the elongation zone was also markedly lower in *mcr1* roots (Figure 1(e)). By contrast, the cortical cells in the meristematic and elongation zones were larger in *mcr1* roots than in wild type (Figures 1(f) and S1(a)). These results suggested that the short root phenotype of the *mcr1* mutant reflected changes in the activity of the RAM.

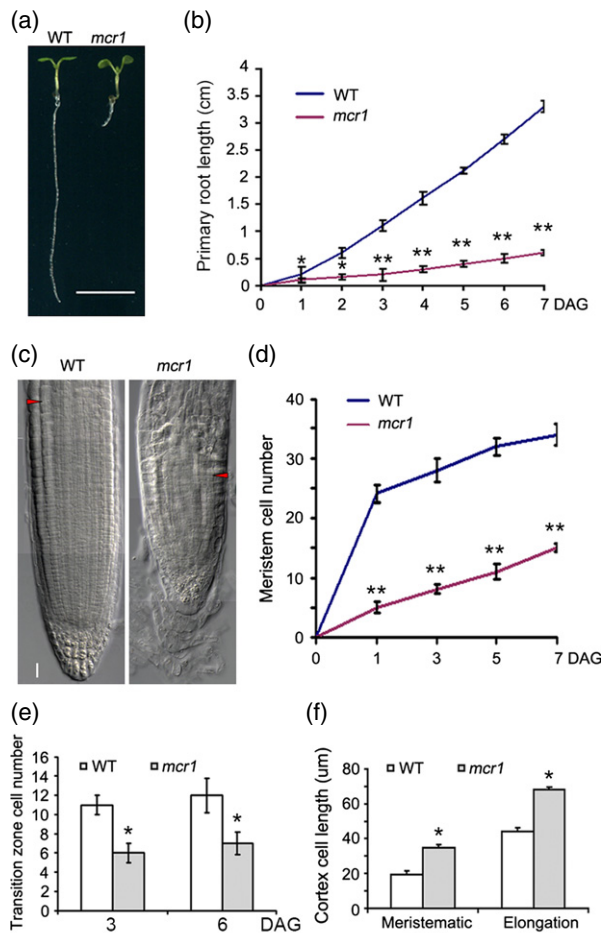


**Figure 1.** *mcr1* shows reduced root meristem size and stunted root growth. (a) Phenotype of WT (Col-0) and *mcr1* seedlings at 6 DAG. Bar = 16 mm. (b) Primary root length of WT and *mcr1* seedlings from germination to 7 DAG. The data shown are means  $\pm$  standard deviation (SD) ( $n = 30$ ). (c) Photograph of the root meristematic zone in WT and *mcr1* plants at 6 DAG. Bar = 20  $\mu$ m. (d) Root meristem cell number in WT and *mcr1* plants from 1 to 7 DAG. The data shown are means  $\pm$  SD ( $n = 30$ ). (e) Cell numbers in the elongation zone of WT and *mcr1* plants at 3 and 6 DAG. The data shown are means  $\pm$  SD ( $n = 30$ ). (f) Cortical cell size in WT and *mcr1* plants in the meristem and elongation zones at 6 DAG. The data shown are means  $\pm$  SD ( $n = 30$ ). Asterisks in (b), (d), (e) and (f) denote significant differences by Student's *t*-test compared with WT (\* $P < 0.05$ ; \*\* $P < 0.01$ ).

To test whether the *mcr1* mutant has reduced root meristematic activity, we measured the rate of mature epidermal cell production between 3 and 10 DAG. We found that the cell production rate in both mutant and wild type (WT) roots was relatively constant over a period of 10 days. Wild type produced approximately 30 cells per day, and the average length of cells was about 135  $\mu$ m (Figure S1(b, c)). In sharp contrast, *mcr1* produced only about eight cells per day with an average cell length of about 100  $\mu$ m (Figure S1(b, c)) suggesting altered regulation of cell division in the RAM. Furthermore, the size of cortical cells in mature zone in *mcr1*

roots was reduced by 36% compared to wild type (Figure S1(d)). Intriguingly, we found that the primary root growth rate in *mcr1* declined rapidly and essentially ceased at 4 weeks after stratification (Figure S1(e)). In parallel, the size of RAM in the mutant decreased sharply, and the RAM became barely visible upon 4 weeks (Figure S1(f)). Taken together, these results indicated that *MCR1* is essential for the maintenance of RAM size and root meristematic activity.

#### *mcr1* is a new allele of *prl1*

To identify the *mcr1* locus, a genomic fragment flanking the left border of the T-DNA insertion in the mutant was isolated by thermal asymmetric interlaced-polymerase chain reaction (TAIL-PCR). Subsequent BLAST search with the plant DNA–T-DNA junction sequence revealed that the T-DNA was inserted into intron 14 of *PRL1* (Figures 2(a) and S2(a)). Further assays showed that primary root growth in the *mcr1* plants was similar that in *prl1-1* (Figure 2(b)). To confirm whether the T-DNA insertion in *PRL1* was responsible for the short root phenotype, an allelism test was performed by crossing homozygous *mcr1* and *prl1-1* mutants. The short root phenotype and all other phenotypic traits of the F1 offspring were indistinguishable from those previously described and observed in *prl1* (Németh *et al.*, 1998), demonstrating that the *mcr1* mutation represented a new *prl1* allele (Figure 2(b)). Furthermore, the root length of *mcr1* mutant carrying a genomic *PRL1*–*GFP* fusion (*gPRL1*–*GFP*) construct introduced into *mcr1* by crossing showed similar root length as WT, indicating genetic complementation of the *mcr1* mutation (Figure S2(b)). Thereafter, *mcr1* was renamed as *prl1-9* (Flores-Perez *et al.*, 2010). Upon backcross of *prl1-9* with WT (Col-0), the F2 yielded 717 WT and 262 *prl1-9* progeny with short roots indicating a 3:1 segregation ( $\chi^2 = 1.66 < 3.841$ ; chi-square test with one degree of freedom). Reverse transcription (RT)-PCR assays indicated that 3'-region of the truncated *prl1-9* allele was transcribed as expected and described for the *prl1-1* mutant (Figure 2(c)), in which a T-DNA insertion in exon 15 was previously demonstrated to prevent the production of immunologically detectable C-terminally truncated PRL1 protein product (Németh *et al.*, 1998).

#### The *prl1-9* mutant is defective in G1/S and G2/M cell cycle transitions

To investigate whether cell cycle progression in the RAM was altered in *prl1-9*, we compared the expression patterns of several cell cycle-related genes in the root tips of *prl1-9* and WT seedlings by quantitative qRT-PCR. Among those tested, the plant-specific cyclins *CycD1;1*, *CycD2;1*, and *CycD3;1* play roles in the G1/S phase transition of the cell cycle (Menges *et al.*, 2005; de Jager *et al.*, 2009). The result showed that transcription of *CycD1;1* and *CycD3;1* was markedly decreased in *prl1-9* root tips compared to WT

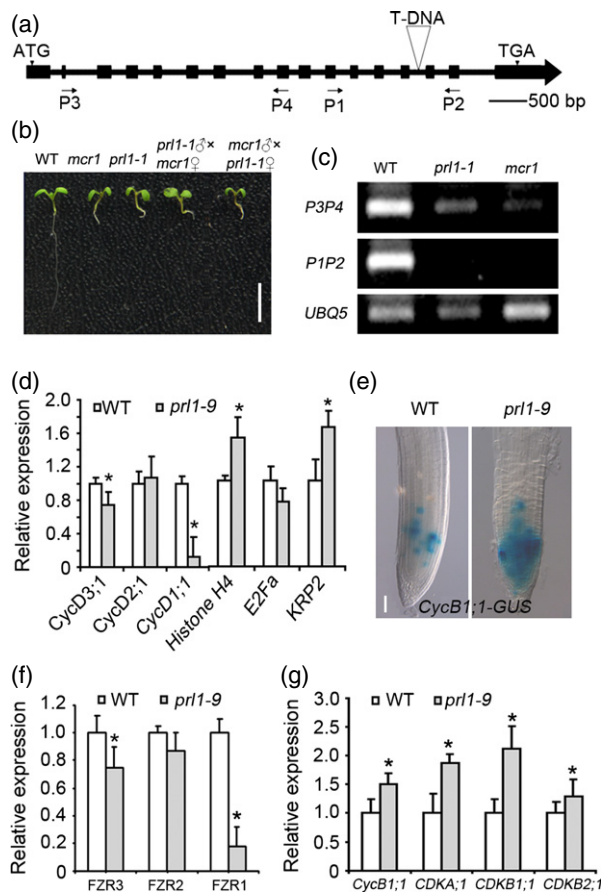


**Figure 2.** *MCR1* encodes PRL1 and modulates cell cycle progression. (a) *PRL1/MCR1* gene structure. The start (ATG) and stop (TGA) codons are indicated. Black boxes indicate exons. Lines between boxes indicate introns. (b) Phenotype analysis of F1 generation of double mutant (*mcr1* $\sigma$   $\times$  *prl1-1* $\sigma$  and *prl1-1* $\sigma$   $\times$  *mcr1* $\sigma$ ) at 6 DAG. Bar = 1 cm. (c) RT-PCR analysis of *PRL1* expression. P1, P2, P3, and P4 denote the positions of the primers in (a). (d, f, g) Quantitative real-time RT-PCR analysis of cell cycle-related gene expression in *prl1-9* mutant root tip. *UBQ5* was used as a reference. The values are given as means  $\pm$  standard deviation (SD) (\* $P$  < 0.05, *t*-test). (e) *CycB1;1:GUS* expression in WT and *prl1-9* plants at 6 DAG. Bar = 30  $\mu$ m.

(Figure 2(d)), whereas the level of *CycD2;1* was unchanged (Figure 2(d)). We next analyzed the expression of genes encoding Kip-related proteins (KRPs), which are inhibitors of cyclin-dependent kinase (CDK) activity that negatively regulate the G1/S transition (De Veylder *et al.*, 2001). We found that *KRP2* was upregulated in *prl1-9* (Figure 2(d)). Expression of the *histone H4* gene, which is usually used as a marker of S phase cells, was elevated in *prl1-9* root tips compared with wild type, whereas the expression of *E2Fa*, active at the G1/S transition, was slightly decreased in *prl1-9* (Figure 2(d)).

Next, we examined whether the *prl1-9* mutation would also affect the G2/M phase transition. First, we analyzed the expression level of mitotic cyclin *CycB1;1* in *prl1-9* by

crossing the mutant with a transgenic line expressing *CycB1;1:GUS* (Colon-Carmona *et al.*, 1999; Donnelly *et al.*, 1999). Histochemical staining showed that the GUS activity was dramatically higher in *prl1-9* root meristem compared to WT (Figure 2(e)), suggesting that the cell cycle in *prl1-9* RAM was slowed down at the G2 to M phase transition. It is known that *CycB1;1* transcription is activated in G2 phase, and *CycB1;1* is degraded by the anaphase-promoting complex/cyclosome activator (APC/C) complex at metaphase (Zheng *et al.*, 2011), APC/C complex contains at least 11 different subunits (APC1–APC11), including the catalytic core subunits APC2 and APC11, and among them, activation and substrate specificity of APC2 and APC11 are regulated by the Fizzy-related (FZR) proteins. In Arabidopsis, there are three FZR homolog genes (*FZR1*, *FZR2*, *FZR3*) (Bao *et al.*, 2012). qRT-PCR analysis showed that the transcription levels of FZR genes were reduced in *prl1-9* (Figure 2(f)), while the *CycB1;1* mRNA level was increased (Figure 2(g)), consistent with the GUS staining results. We also examined the transcript levels of plant-specific cell cycle kinase genes *CDKA;1* and *CDKBs* (Figure 2(g)), whose expression is strictly regulated during the cell cycle and is increased between S and M phase. The expression of *CDKA;1*, which is expressed throughout the cell cycle (Van-dopoele *et al.*, 2002; Menges *et al.*, 2005), was increased in *prl1-9*. Transcript levels of *CDKB1;1* and *CDKB2;1*, which are expressed from S to early M phase and from G2 to M phase, respectively (Segers *et al.*, 1996; Umeda *et al.*, 1999; Menges *et al.*, 2002), were also markedly higher in *prl1-9* compared to WT (Figure 2(g)). We further examined the mitotic index in the RAM of *prl1-9* and found that there were fewer mitotic figures (metaphase, anaphase, and telophase) in the RAM of *prl1-9* than in WT plants (Figure S3). In conclusion, these results indicated that the *prl1-9* mutation reduced the expression levels of several G1/S specific transcripts while increasing the expression levels of G2/M phase-specific marker genes suggesting a potential defect in G2/M phase transition.

### ***PRL1* is expressed in the RAM of primary roots and affects the control of RAM size**

To examine in more details the role of *PRL1* in root development, we analyzed the expression pattern of a *PRL1* promoter–GUS reporter (*PRL1pro:GUS*) during root development. Activity of *PRL1pro:GUS* was detectable in radicles of germinating seeds as early as 12 h after germination (Figure 3(a)). Strong GUS activity was further detectable in the root apical regions of germinating seedlings at 2 to 3 days after stratification, especially in the apical meristems of primary roots (Figure 3(b, c)). In young seedlings, the GUS activity was prominent in the RAM (Figures 3(d–f)). The cell- and tissue-specific expression of *PRL1* during primary root growth indicates its role in establishing and maintaining the RAM during root development.

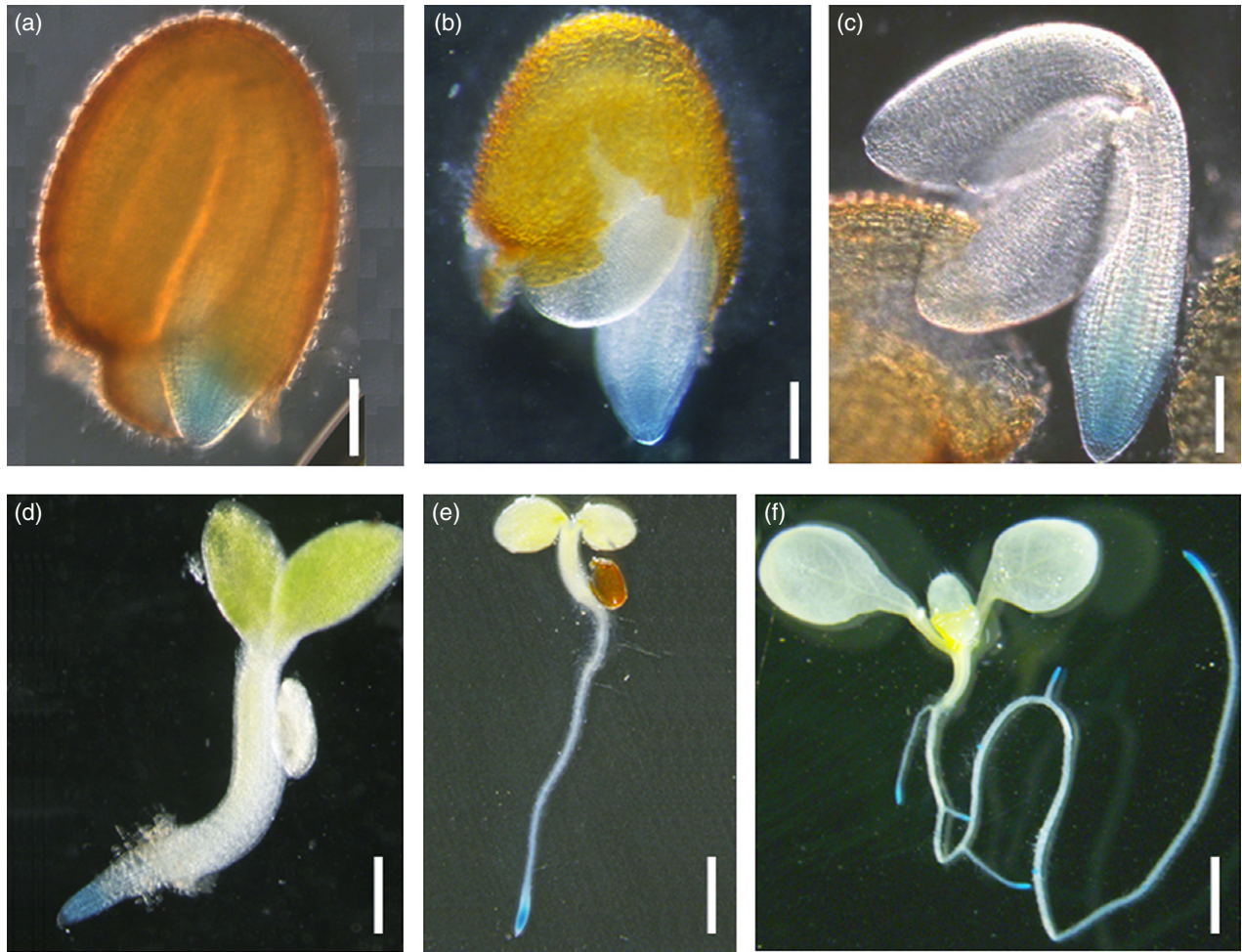


**Figure 3.** Analysis of the *PRL1* expression pattern in root tip.

*PRL1pro:GUS* transgenic seeds were grown on MS medium for (a) 12 h (Bar = 120  $\mu$ m), (b) 2 DAG (Bar = 120  $\mu$ m), (c) 3 DAG (Bar = 150  $\mu$ m), (d) 5 DAG (Bar = 300  $\mu$ m), (e) 7 DAG (Bar = 500  $\mu$ m), and (f) 12 DAG (Bar = 500  $\mu$ m) before GUS staining assays.

Next, we investigated how auxin treatment affects *PRL1* expression in the root. *PRL1pro:GUS* seedlings were treated with 0.1 nM and 5  $\mu$ M indole-3-acetic acid (IAA) as described previously (Peng *et al.*, 2013). The expression of *PRL1pro:GUS* in the RAM was not significantly affected by the application of 0.1 nM IAA at 5 h after treatment, and was also only marginally reduced by treatment with 5  $\mu$ M IAA (Figure 4(a)). This was further confirmed by qRT-PCR measurements of *PRL1* mRNA levels in the roots of 6-day-old seedlings (Figure 4(b)). In transgenic *prl1-9* mutant plants carrying a complementing genomic *PRL1-GFP* fusion (*gPRL1-GFP*) construct, the GFP fluorescence localized in nuclei of root cells (Figure 4(c)) was similarly to WT and only marginally reduced by 5  $\mu$ M IAA treatment (Figure 4(d)). These results indicated that auxin does not modify remarkably transcriptional and post-transcriptional regulation of *PRL1*. Nonetheless, the *prl1-9* mutation appeared to reduce auxin-stimulated increase of the root meristem size. Exogenous application of 0.1 nM IAA to

roots of 6-day-old WT and *prl1-9* seedlings for 24 h resulted in a 23.2% increase in the number of root meristem cells in WT roots, but only a 12.5% increase in *prl1-9* (Figure 4(e, f)). When treated with 5  $\mu$ M IAA, the size of the root meristem in WT was reduced by 14.8% compared with 6.3% in *prl1-9* (Figure 4(e, g)). Consequently, these results indicated that the *prl1-9* mutation compromises auxin-dependent control of the root meristem size.

#### **The *prl1-9* mutation alters auxin distribution and PIN expression levels in the roots**

To investigate whether the *prl1-9* mutation alters normal auxin distribution in the roots, we compared the expression pattern of auxin-responsive *DR5:GUS* reporter (Ulmasov *et al.*, 1997; Blilou *et al.*, 2005) in mutant and WT seedlings. As shown in Figure 5(a, b), the expression pattern of *DR5:GUS* reporter was considerably reduced in the *prl1-9* mutant compared with WT suggesting that the mutation altered auxin maximum in the root apex. To

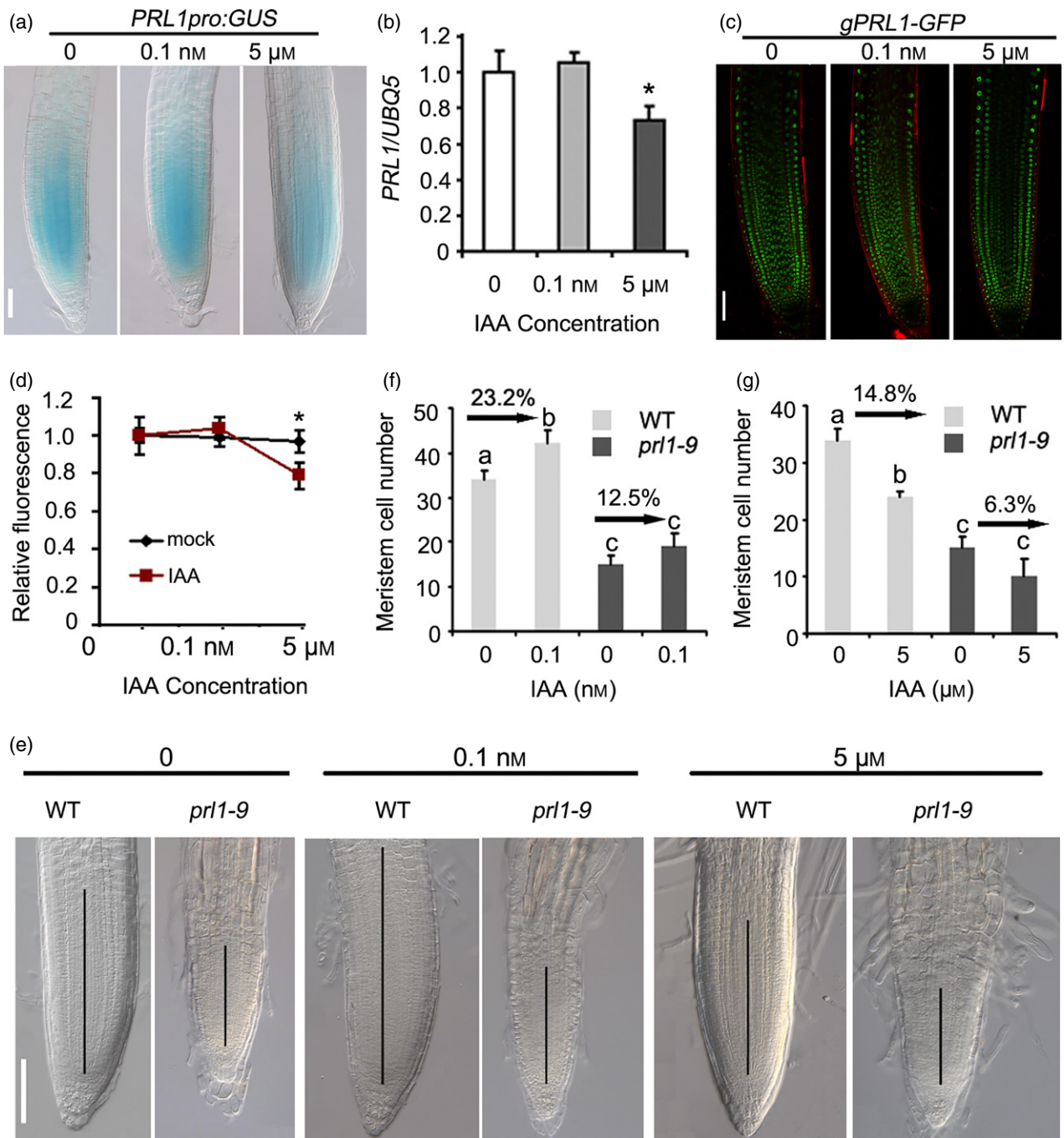


**Figure 4.** Auxin influences *PRL1* gene and protein expression. (a) *PRL1pro:GUS* transgenic seedlings (6 DAG) were treated with 0.1 nM or 5 μM IAA for 5 h before GUS staining assays. Bars = 50 μm. (b) Quantitative real-time analysis of auxin-regulated *PRL1* expression in wild type. Seedlings (6 DAG) were treated with 0.1 nM or 5 μM IAA for 5 h. The values given are means ± standard deviation (SD) (\**P* < 0.05, *t*-test). (c) *gPRL1-GFP* transgenic seedlings (6 DAG) were treated with 0.1 nM or 5 μM IAA for 5 h, respectively, before GFP assays. (d) Fluorescence quantification of auxin-treated *gPRL1-GFP* from (c). The intensity values detected by confocal were compared with untreated wild type (set at 1.0). The values given are means ± SD (\**P* < 0.05, *t*-test). (e) Root meristem tissues of 6-day-old WT or *prl1-9* seedlings treated with 0.1 nM or 5 μM IAA for 24 h, respectively. Black vertical lines represent the length of the meristem. (f, g) Average number of cortical cells in root meristems of 6-day-old WT or *prl1-9* seedlings from (e). The values given in (f) and (g) are means ± SD. <sup>a,b,c</sup>Different letters shows the significant differences with one-way analysis of variance (ANOVA) (*P* < 0.05). Bars = 80 μm.

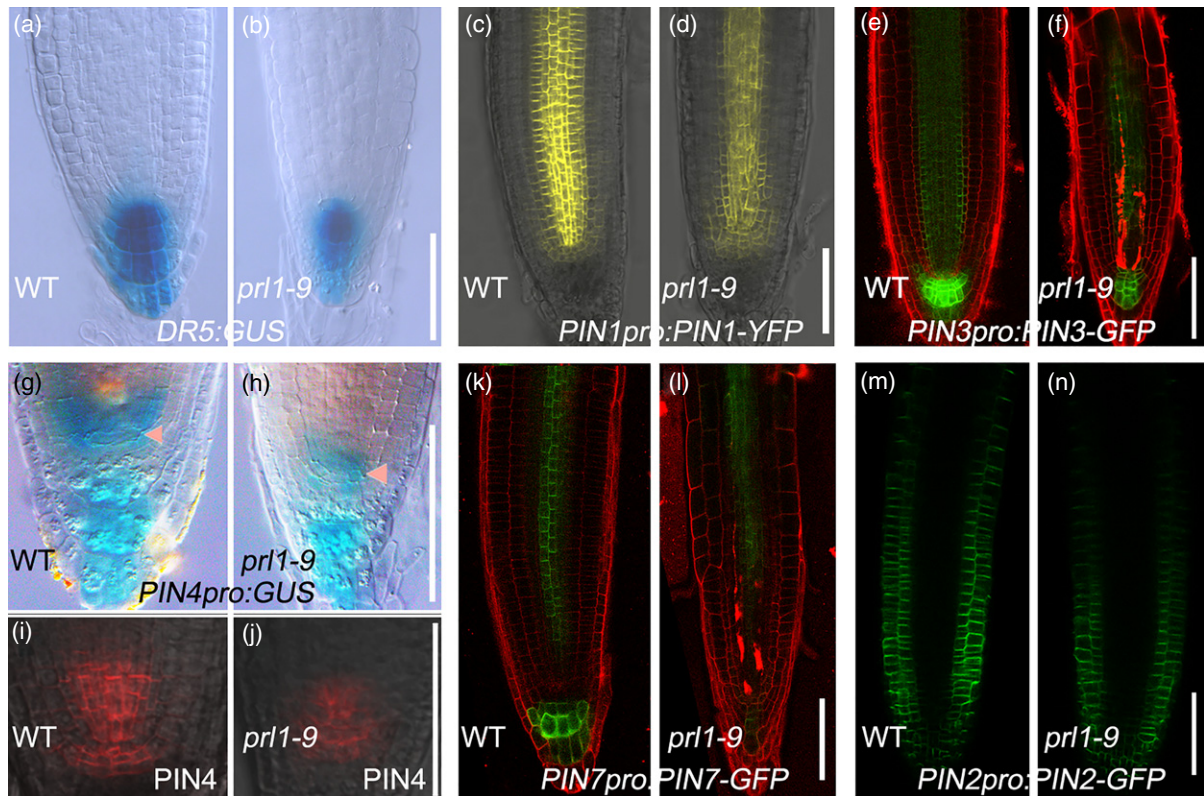


**Figure 5.** The mutation of *PRL1* affects auxin maximum and PINs expression level.

(a, b) Expression patterns of the *DR5:GUS* reporters in WT (a) and *prl1-9* (b) plants at 6 DAG.

(c, d) *PIN1pro:PIN1:YFP* expression in WT (c) and *prl1-9* (d) plants at 6 DAG.

(e, f) *PIN3pro:PIN3:GFP* expression in WT (e) and *prl1-9* (f) plants at 6 DAG.

(g, h) *PIN4pro:GUS* expression in WT (g) and *prl1-9* (h) plants at 6 DAG. Arrowheads denote QC cells.

(i, j) The protein level of PIN4 in WT (i) and *prl1-9* (j) plants at 6 DAG using immunohistological method with the PIN4 antibody.

(k, l) *PIN7pro:PIN7:GFP* expression in WT (k) and *prl1-9* (l) plants at 6 DAG.

(m, n) *PIN2pro:PIN2:GFP* expression in WT (m) and *prl1-9* (n) plants at 6 DAG. Bars = 100  $\mu$ m.

determine whether the *prl1-9* mutation would influence the localization or expression of the PIN auxin efflux carriers, we generated *prl1-9* plants expressing PINs in fusion with GFP/YFP reporters under the control of their native promoters by genetic crosses. The activity of *PIN1pro:PIN1-YFP* was markedly reduced in the vascular tissue (Blilou *et al.*, 2005; Dello loio *et al.*, 2008), but showed an extended pattern in the transition zone proximal to the stem cell region in *prl1-9* compared with WT (Figure 5(c, d)). The expression levels of *PIN3pro:PIN3-GFP* and *PIN7pro:PIN7-GFP* (Friml *et al.*, 2002b; Dello loio *et al.*, 2008) were markedly lower in the columella cells, as well as the vascular issues, in *prl1-9* roots (Figure 5(e, f, k, l)). Remarkably, the *prl1-9* mutation diminished the expression of *PIN4pro:GUS* (Figure 5(g, h)) and PIN4 protein (Figures 5(i, j)) in the root stem cell niche suggesting a potential correlation with altered auxin regulation of cell proliferation in *prl1-9* roots. We also examined the *DR5:GUS* expression in cotyledons in *prl1-9* and found that *DR5:GUS* expression in *prl1-9* was also reduced compared with the WT (Figure S4), indicating that the reduced auxin maximum in root meristem of *prl1-*

9 is not due to the reduced activity of PIN1, PIN3, PIN4 and PIN7. In accordance with profound inhibition of root elongation by the *prl1-9* mutation, the expression pattern of *PIN2pro:PIN2-GFP* was confined to a reduced region of differentiation and elongation zones compared with wild type, but its pattern was unaffected by the *prl1-9* mutation (Figure 5(m, n)). The observed shift in auxin distribution and missing PIN4 accumulation in the root stem cell niche, along with inhibition of auxin-dependent changes in the cell number in the *prl1-9* mutant, indicated that PRL1 is required for proper control of RAM maintenance and functioning.

#### **PRL1 confines *WOX5* expression in the QC and QC identity**

Regulation of activity of root stem cell niche is a crucial determinant of root meristem size (Aida *et al.*, 2004; Della Rovere *et al.*, 2013). Therefore, we examined how the *prl1-9* mutation affects the activity of stem cell niche. To test this, the expression patterns of several cell type-specific marker genes in the stem cell niche were analyzed. *QC25:GUS*, which is specifically expressed in the QC of WT

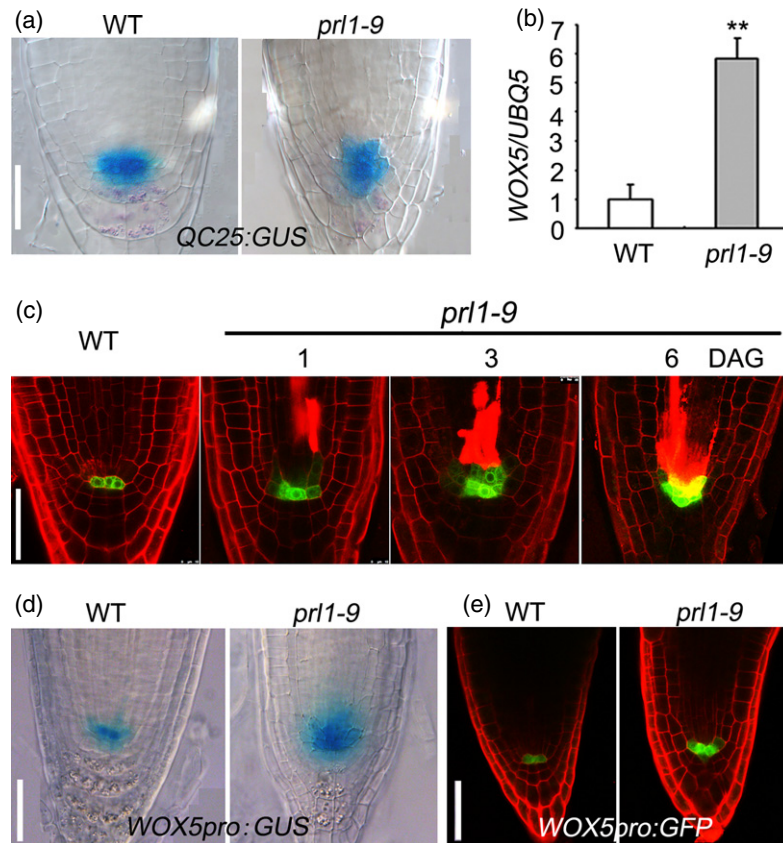


**Figure 6.** *prl1-9* affects stem cell niche activity.

(a) Double staining for the *QC25:GUS* reporter (blue) and starch granules (brown) in WT and *prl1-9* plants at 6 DAG. Bars = 50  $\mu$ m.

(b) Quantitative real-time PCR analysis of *WOX5* expression in WT and *prl1-9* plants. The values given are means  $\pm$  standard deviation (SD). Asterisks denote significant differences by Student's *t*-test compared with WT (\**P* < 0.05).

(c) *WOX5pro:GFP* expression pattern in WT and *prl1-9* plants at 1, 3 and 6 DAG. Bars = 50  $\mu$ m.

(d) *WOX5pro:GUS* expression pattern in WT and *prl1-9* plants at 6 DAG. Bars = 50  $\mu$ m.

(e) *WOX5pro:GFP* expression pattern in WT and *prl1-9* plants at the mature embryo stage. Bars = 50  $\mu$ m.

(Sabatini *et al.*, 1999), showed extended expression in the lower layer of columella initials (termed also columella stem cells, CSC) and in the upper layer of proximal (provascular) stem cells (PSCs) in the *prl1-9* mutant (Figure 6(a)). In addition, disorganized QCs were frequently observed. Their frequency was only 8% in wild type ( $n = 80$ ; at 6 DAG), whereas in *prl1-9* it reached as high as 67% ( $n = 80$ ; at 6 DAG). These results clearly indicated that the QC cells were mitotically active in *prl1-9*.

The expression of *WOX5* in QC is critical for maintenance of the stem cell niche (Sarkar *et al.*, 2007). Therefore, we tested whether *WOX5* expression was altered by the *prl1-9* mutation. In fact, we observed five times higher *WOX5* transcript levels in primary roots of 6-day-old *prl1-9* seedlings compared with WT (Figure 6(b)). To confirm this finding, we examined the expression pattern of a *WOX5pro:GFP* during early development of mutant and WT roots. In WT, *WOX5* expression was confined to the QC cells and it was maintained at a stable level throughout the first 6 days of germination (Figure 6(c)).

In comparison, we observed considerably higher *WOX5pro:GFP* expression in the QC of *prl1-9* already 1 day after germination, and *WOX5pro:GFP* levels continued to increase up to six DAG. More importantly, ectopic *WOX5pro:GFP* expression was clearly detectable in the PSC stem cell layer proximal to the stem cell niche (Figure 6(c)). As further confirmation, the same pattern of *WOX5* activity was observed using a *WOX5pro:GUS* reporter (Figure 6(d)). Remarkably, an extension of *WOX5pro:GFP* expression to the QC-adjacent lateral cells was already observable in *prl1-9* embryonic roots (Figure 6(e)). *WOX5* expression was ultimately decreased and diminished only about 4 weeks after germination, when root growth ceased (Figure S5). Taken together, these data demonstrated that a failure to maintain proper *WOX5* homeostasis and QC cell-specific expression resulted in abnormal (i.e., increased) RAM activity in the *prl1-9* mutant indicating that PRL1 is required for proper control of the dose of *WOX5* in QC and thereby for maintenance of normal QC.



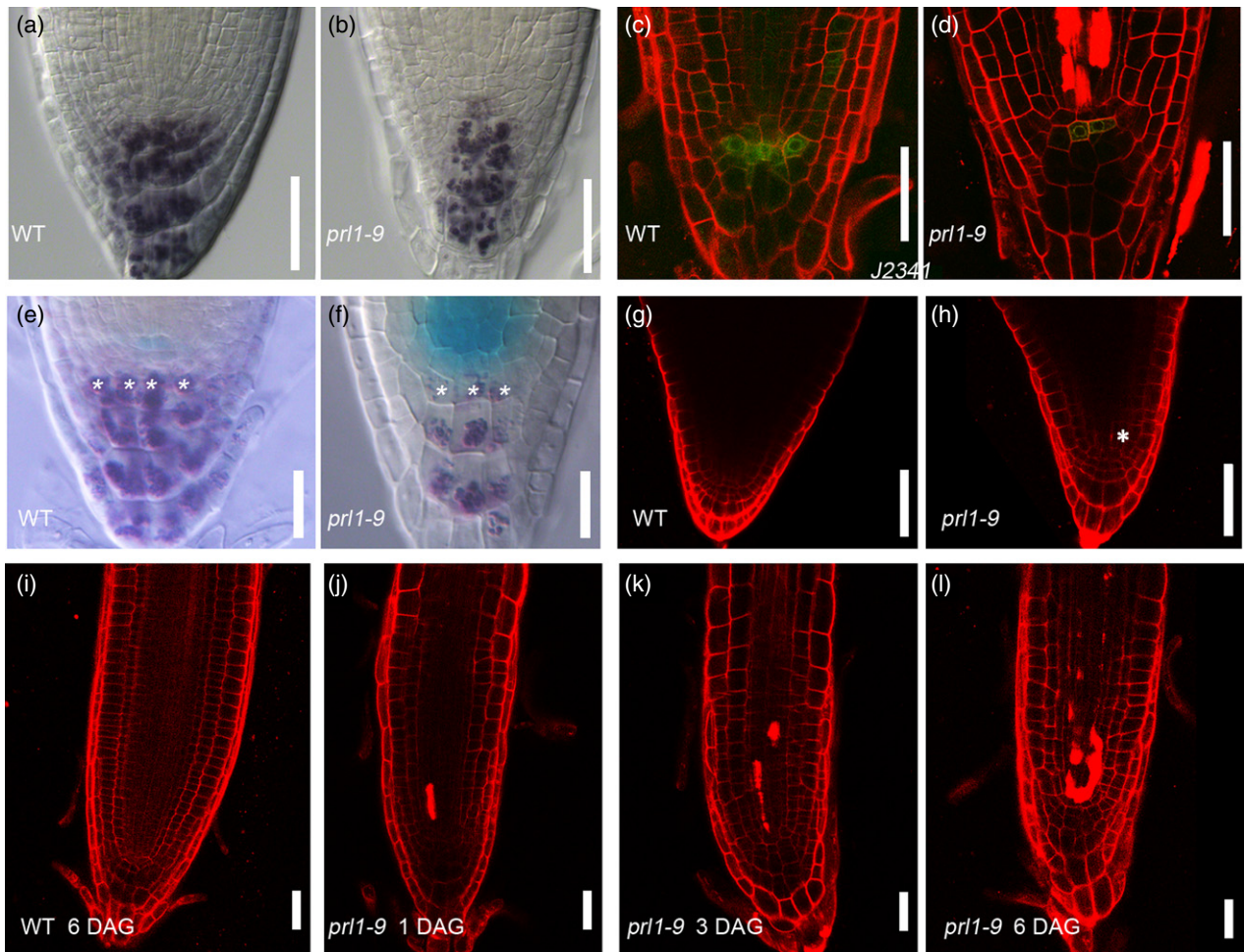


**Figure 7.** *prl1-9* affects distal and proximal stem cell activity. (a, b) I-KI staining of WT (a) and *prl1-9* (b) plants at 6 DAG. (c, d) Expression pattern of *J2341* in WT (c) and *prl1-9* (d) plants at 6 DAG. (e, f) Expression pattern of *WOX5pro:GUS* in WT (e) and *prl1-9* (f) plants at 6 DAG. \*Denotes the columella cells. (g, h) PI staining of the radicle in WT and *prl1-9* plants at 12 h imbibition in water. \*Denotes the differentiated cells. (i-l) PI staining of WT and *prl1-9* plants at indicated times. Bars = 50  $\mu$ m.

### **PRL1 modulates the differentiation of distal and proximal stem cells**

The QC is an organizing center that is required for maintenance of initial root cell division and differentiation (van den Berg *et al.*, 1997). As QC specification was compromised in *prl1-9*, we investigated whether CSC and PSC activities were also affected. In WT, a single layer of CSCs was present between the QC and differentiated columella cells marked by starch granules (Figure 7(a)). Whereas in WT only  $5 \pm 1.4\%$  of cells ( $n = 80$ ) corresponding to the CSC layer showed starch granule accumulation, in the *prl1-9* mutant  $69 \pm 4.1\%$  of cells in this layer accumulated starch ( $n = 80$ ; *t*-test,  $P < 0.05$ ; Figure 7(a, b)). Nonetheless, the expression of CSC-specific marker *J2341* was strongly suppressed in *prl1-9* (Figure 7(c, d)), and accordingly the number of columella cell layers was reduced (Figure 7(e,

f)). This supported the conclusion that *PRL1* is required for the maintenance of CSC activity.

Next, we used propidium iodide (PI) staining to examine whether premature PSC differentiation occurred in the proximal region of the QC. As shown in Figure 7(g, h), one or two PSCs were strongly stained by PI in *prl1-9* versus WT plants already at the embryo stage. More provascular cells were stained starting from 1 to 6 DAG, and the PI-stained cells expanded toward the PSCs until nearly all of the PSCs in the proximal meristem were stained ( $1 \pm 0.4\%$  in WT,  $n = 80$ ;  $98 \pm 0.6\%$  in *prl1-9*,  $n = 80$ ; *t*-test,  $P < 0.01$ ) (Figure 7(i-l)). This result indicated that the PSCs of mutant roots differentiated prematurely into vascular tissues. Based on these data, we concluded that *PRL1* controls the maintenance and status of both PSC and CSC.

### **PRL1 modulates stem cell niche activity and meristem size via a PLT1/PLT2 dependent pathway**

The *PLT* pathway modulates auxin-dependent maintenance of stem cell niche (Sabatini *et al.*, 2003; Aida *et al.*, 2004). To ascertain the genetic relationship between *PRL1* and *PLT* in regulating stem cell niche activity, we generated a *prl1-9plt1-4plt2-2* triple mutant by crossing *prl1-9* with *plt1-4plt2-2* and subsequently analyzed the size of the RAM in *prl1-9*, *plt1-4plt2-2*, and *plt1-4plt2-2prl1-9* plants. The size of the root meristem in *prl1-9* was significantly larger than that in *plt1-4plt2-2*. Notably, the size of the root meristem in the *plt1-4plt2-2prl1-9* triple mutant was identical to that of the *plt1-4plt2-2* double mutant (Figure 8(a, b)) indicating that *PRL1* functions upstream of *PLT1/PLT2* in the regulation of RAM size.

To confirm the relationship between *PRL1* and *PLT1/PLT2*, we analyzed the influence of the *prl1-9* mutation on the expression of *PLT1* and *PLT2* by examining the activities of *PLT1pro:PLT1-GFP* and *PLT2pro:PLT2-GFP* reporters in *prl1-9*. The protein expression levels of both *PLT1* and *PLT2* were remarkably reduced in *prl1-9* compared with WT (Figure 8(c, d)), we also examined the transcription level of *PLT1* and *PLT2* in the mutant and found that *PLT1* and *PLT2* genes were also reduced in *prl1-9* compared with WT (Figure S6). The results indicated that *PRL1* is required for maintenance of normal *PLT1* and *PLT2* levels. To validate this conclusion, we have introduced a *PLT2* overexpression construct *35Spro:PLT2-GR* into the *prl1-9* mutant. As shown in Figure 8(e), the size of the meristem in WT plants expressing *35Spro:PLT2-GR* was significantly increased after induction with dexamethasone (DEX) (Figure 8(e, f)), consistent with a previous report (Galinha *et al.*, 2007). When treated with DEX, the meristem size of *prl1-9* expressing *35Spro:PLT2-GR* was also increased to a level comparable with that seen in WT (Figure 8(e, f)). Complementation of the *prl1-9* root meristem phenotype by overexpression of *PLT2* suggests that *PRL1* acts upstream of *PLT1/PLT2* in the regulation of root meristem size.

As *WOX5* and *PLTs* act in concert with *SHORT-ROOT* (*SHR*) and *SCARECROW* (*SCR*) to control QC identity, we also generated *scr-1 prl1-9* and *shr-2 prl1-9* double mutants and analyzed their root meristem sizes. The meristems in both *scr-1prl1-9* and *shr-2prl1-9* were significantly smaller than those of individual *scr-1*, *shr-2*, or *prl1-9* mutants suggesting an additive effect of these mutations (Figure S7(a, b)). Further examination of *SHRpro:SHR-GFP* and *SCRpro:SCR-GFP* activities in *prl1-9* revealed that the expression patterns of both reporter genes were unaltered (Figure S7(c, d)). This ultimately showed that *PRL1* functions independently of the *SHR/SCR* pathway in regulating root meristem size.

### **DISCUSSION**

Recent studies have identified several key determinants that specify the stem cell niche and prevent the differentiation of stem cells in the root stem cell niche. These determinants have led to the discovery of the *PLT* dependent pathway, which functions downstream of auxin and modulates auxin-mediated root meristem control (Aida *et al.*, 2004). However, the mechanism that modulates the root stem cell niche maintenance is not yet fully understood. Here, we found that *PRL1* is an upstream regulator of the *PLT1/PLT2* dependent pathway that modulates root meristem size and stem cell niche maintenance.

In a genetic screen for novel root meristem mutations we identified the Arabidopsis *mcr1* mutant that exhibited defects in the root meristem displaying short roots. The *mcr1* mutant was found to carry a T-DNA insertion in the *PRL1* gene (Figure 2(a)). *PRL1* encodes a WD40-repeat protein subunit of the NTC complex and has long been recognized as a central regulator of transcription, splicing and numerous plant developmental, hormonal and stress signaling pathways (Németh *et al.*, 1998). Although it has been noticed that the *PRL1* expression level was highest in roots and that the *prl1* mutant develop short roots (Németh *et al.*, 1998), the role of *PRL1* in root growth remained so far uncharacterized. We found that loss of the *PRL1* function in the *mcr1/prl1-9* mutant caused a substantial reduction in the size of the RAM (Figure 1(c, d)). Intriguingly, the number of mature epidermal cells in *prl1-9* was much smaller than in WT (Figure S1(c)). Thus, we speculated that the short root phenotype of *prl1-9* was largely due to reduced cellular proliferation in the root. This prediction was shown to be correct based on the observation of disturbed cell cycle progression affecting both G1/S and G2/M transitions in the root meristem of *prl1-9* (Figures 2(d-f) and S3). Taking into consideration that *PRL1* was expressed at the highest level in the meristematic zone of emerging radicals and primary roots (Figure 3), we concluded that *PRL1* is required for proper control cell proliferation in the root meristem, and for root meristem maintenance.

The distribution and maximum level of auxin determine the identity of the stem cell niche and differentiation of stem cells in the root meristem (Ding and Friml, 2010). We found that *PRL1* transcript levels are only marginally reduced by auxin (Figure 4(a-d)). Nonetheless, the cell division response of the root meristem to low and high level of auxin markedly differs from wild type in *prl1-9* mutant (Figure 4(e-g)). This supports the conclusion that *PRL1* modulates the auxin responsiveness of root meristematic cells. The *prl1-9* mutation reduces the expression levels of *PIN1*, *PIN3*, *PIN4*, and *PIN7* auxin efflux carriers (Figure 5(c-n)). In particular, abolishment of *PIN4* gene and *PIN4* protein expression in the *prl1-9* mutant could promi-

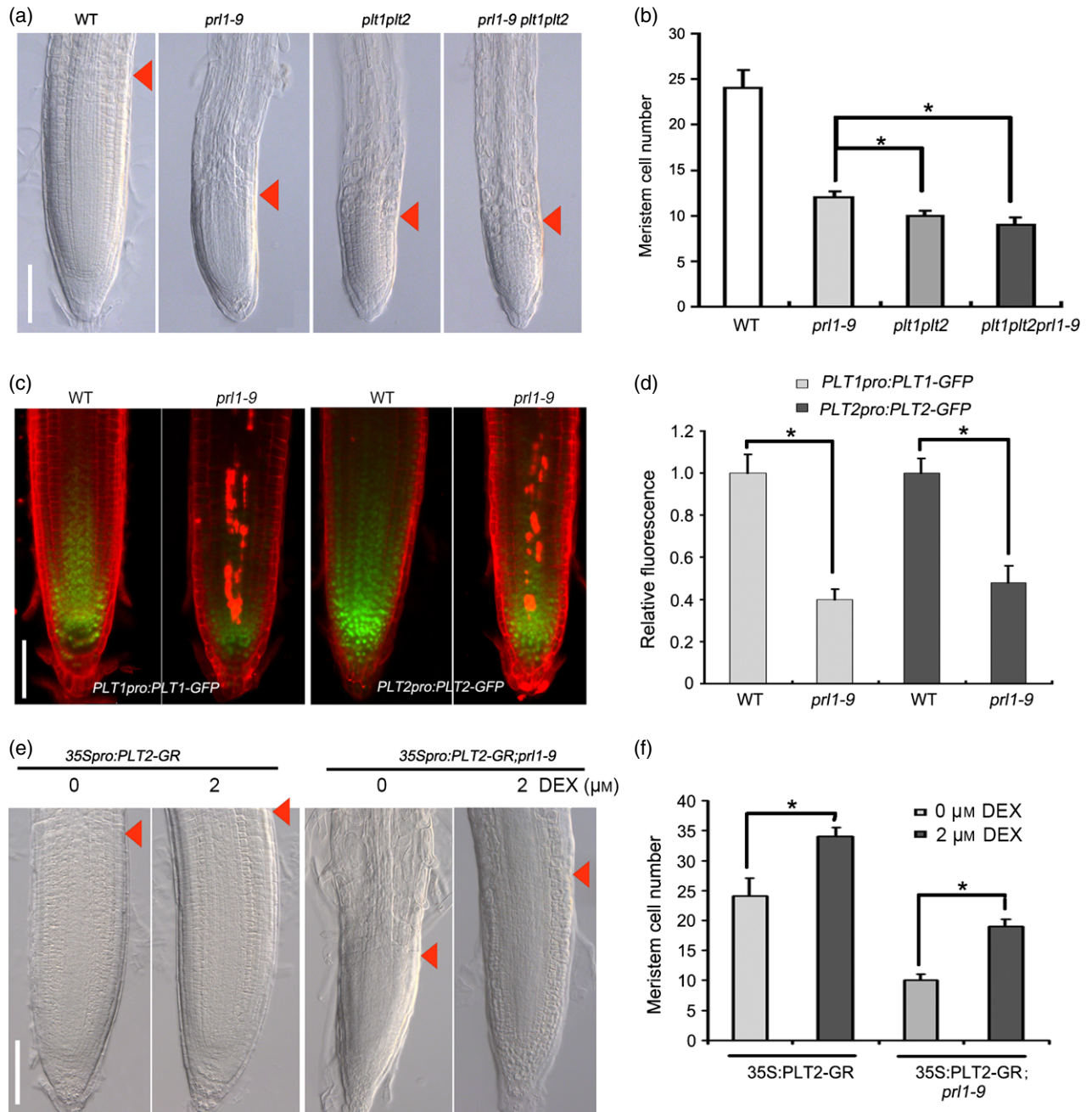


**Figure 8.** PRL1 acts upstream of PLT1/PLT2 to modulate meristem size.

(a) Root meristem size in *prl1-9* and *plt1-4 plt2-2* single, double, and triple mutants. Red arrowheads indicate the cortex transition zone. Bars = 100  $\mu\text{m}$ .

(b) Average number of cortical cells in the root meristem of WT, *prl1-9*, *plt1-4 plt2-2*, and *plt1-4plt2-2prl1-9* plants at 4 DAG. Meristem cell numbers for the indicated genotypes at 4 DAG. The data shown are means  $\pm$  standard deviation (SD) ( $n = 30$ ) ( $*P < 0.05$ , *t*-test).

(c) *PLT1pro:PLT1:GFP* and *PLT2pro:PLT2:GFP* expression in WT and *prl1-9* root tips at 6 DAG.

(d) Quantification of *PLT1pro:PLT1:GFP* and *PLT2pro:PLT2:GFP* fluorescence as shown in (c). The intensity values detected by confocal were compared with WT (set at 1.0). The values given are means  $\pm$  SD ( $*P < 0.05$ , *t*-test).

(e) Root meristem of *35Spro:PLT2-GR* and *35Spro:PLT2-GR;prl1-9* seedlings were treated with 0 and 2  $\mu\text{M}$  DEX for 2 days.

(f) Average number of cortical cells in root meristem of *35Spro:PLT2-GR* and *35Spro:PLT2-GR;prl1-9* seedlings in (e). The values are given as means  $\pm$  SD ( $*P < 0.05$ , *t*-test) compared with their respective controls. Bars = 100  $\mu\text{m}$ .

nently affect auxin accumulation in the root stem cell niche (Figure 5(g–j)). In fact, we found that inactivation of PRL1 results in derepressed expression of *WOX5* expression in

the QC, as well as in CSCs and PSCs (Figure 6(c)), which is normally repressed in an IAA17-dependent fashion by auxin signaling (Tian *et al.*, 2014). Consistent with the find-

ing that WOX5 overexpression in the QC stimulates auxin synthesis (Tian *et al.*, 2014), we found that expression of the auxin-stimulated reporter *DR5:GUS* reduced in the *prl1-9* mutant compared with WT, indicating a decreased auxin maximum. Furthermore, the *prl1-9* mutation extended the expression of *WOX5* into the cells surrounding the QC and resulted in premature differentiation of both distal CSCs and PSCs in the root meristem (Figures 6(c) and 7(i–l)). This indicated that PRL1 is required for the maintenance of both QC identity and stem cell fate.

It has been established that auxin modulates root meristem size and stem cell niche maintenance by regulating the expression of *PLTs* (Blilou *et al.*, 2005; Grieneisen *et al.*, 2007; Dinneny and Benfey, 2008). Nonetheless, several details of how RAM activity and stem cell niche are controlled by *PLT* dependent signaling remained unknown. In this study, we collected several pieces of evidence demonstrating that PRL1 acts upstream of *PLT1/PLT2* to modulate RAM activity and maintenance of the root stem cell niche. The first piece of evidence derived from an epistasis analysis of *prl1-9* and *plt1plt2* mutations. The root meristem size in the *plt1-4plt2-2prl1-9* triple mutant was identical to that in *plt1-4plt2-2*, instead of that in *prl1-9* (Figure 8(a, b)). Next, we showed that the *prl1-9* mutation reduced *PLT1* and *PLT2* expression in the root meristematic zone (Figure 8(c, d)), and that DEX-induced *PLT2* overexpression resulted in a rescue of the root meristem size defect of *prl1-9* (Figure 8(e, f)). In combination with the analysis of *WOX5* expression in *prl1-9*, we thus demonstrated that PRL1 plays an important role in maintaining the identity of the QC and stem cell activity. Previous studies have shown that *WOX5* is specifically expressed in the QC and that it functions upstream of *PLTs* in distal stem cell maintenance (Ding and Friml, 2010). Auxin represses *WOX5* expression in the root meristem, which in turn regulates the expression of *PLTs*, whose levels determine the fate of distal stem cells (Aida *et al.*, 2004; Sarkar *et al.*, 2007). Consequently, our study defines PRL1 as upstream regulator of *WOX5-PLT* pathway in the control of QC identity and distal stem cell activity. Our data show so far that PRL1 represses *WOX5* expression and activates *PLT1/PLT2* activity, which is essential for maintenance of the QC and distal stem cells. In addition, PRL1 activity is also required for the maintenance of PSCs. However, it remains an important further question how inactivation of PRL1 leads to derepression of *WOX5*, which requires further identification of PRL1 targets in auxin signaling.

## EXPERIMENTAL PROCEDURES

### Plant materials and growth conditions

The *A. thaliana* (L.) seeds used in this study were surface-sterilized with 50% (v/v) commercial bleach for 5 min, followed by five rinses with sterilized water. The seeds were then plated on agar

plates containing MS nutrient mix (PhytoTechnology Laboratories®, Overland Park, KS, USA) supplemented with 1% sucrose and 0.8% agar at pH 5.7. Two days after stratification at 4°C in the dark, the seeds were germinated at 22°C under a 16-h light/8-h dark photoperiod. The wild type accession used in this study is Columbia-0 (Col-0). The *prl1-1* mutant was described by Németh *et al.* (1998). The following types of transgenic seeds were obtained: *SHRpro:SHR-GFP*; *SCRpro:SCR-GFP*; *plt1plt2* (Aida *et al.*, 2004); *PLT1pro:PLT1-GFP* and *PLT2pro:PLT2-GFP* (Matsuzaki *et al.*, 2010); *scr-1* (Di Laurenzio *et al.*, 1996); *shr-2* (Levesque *et al.*, 2006); *WOX5pro:GFP* (Haecker *et al.*, 2004); *WOX5pro:GUS* (Sarkar *et al.*, 2007); *35Spro:PLT2-GR* (Galinha *et al.*, 2007); *J2341* and *QC25:GUS* (Sabatini *et al.*, 1999); *CycB1;1:GUS* (Colon-Carmona *et al.*, 1999); *DR5:GUS* (Ulmasov *et al.*, 1997); *PIN1pro:PIN1:YFP* (Benková *et al.*, 2003); *PIN2pro:PIN2:GFP*, *PIN3pro:PIN3:GFP*, and *PIN7pro:PIN7:GFP* (Blilou *et al.*, 2005); and *PIN4pro:GUS* (Friml *et al.*, 2002a). The *prl1-9* mutation was introduced into transgenic lines and wild type (Col-0) by crossing, and independent homozygous lines carrying the mutations and expressing the reporter genes were identified by PCR screening in combination with GUS staining or following GFP and YFP fluorescence.

### Construction of *PRL1pro:GUS* and *gPRL1-GFP* reporter genes

To construct *PRL1pro:GUS*, first a 7.9 kb *XbaI-SpeI* fragment carrying the *PRL1* gene was cloned from pgcPRL16 (Németh *et al.*, 1998) into pBS to yield pBS-PRL1. Next, an *XbaI-BmgBI* fragment of the *PRL1* gene carrying the 3.5 kb upstream promoter region linked to sequences of the untranslated region (-UTR) and coding region extending to the start of the third exon was inserted into *XbaI-SmaI* sites of the promoter test vector pPCV812 upstream of the *GUS* (*uidA*) coding region to yield the binary vector pPCV812-PRL1PROM harbouring the *PRL1pro:GUS* reporter construct.

The *gPRL1-GFP* reporter construct was assembled in multiple cloning steps. The *PRL1* cDNA PCR amplified with the *XhoI*F and *HASpe* primers was cloned into the *SmaI* site of pBS to yield pBS-PRL1-cDNA-HA. -UTR of PRL1 extending from position -62 to the third exon was isolated from pBS-PRL1 as an *MscI-BmgBI* fragment to replace an *MscI-BmgBI* cDNA fragment of pBS-PRL1-cDNA-HA in pBS-PRL1-2introns-cDNA-HA. The coding region of *PRL1* gene extending from the ATG codon to a *SmaI* site replacing the stop codon was PCR amplified with the primers PSM1 and PSM2 and introduced into the *SmaI* site of pBS resulting in pBS-PRL1-SmaI. Next, the *SmaI-BgIII* fragment of *PRL1* gene from pBS-PRL1-SMA was inserted into *BgIII* and filled-in *SpeI* sites of pBS-PRL1-2introns-cDNA-HA to create pBS-PRL1-2introns-cDNA-Sma. The GFP coding region was PCR amplified with GFP-F and GFP-R primers and inserted into *XbaI-SacI* sites of the latter plasmid to create pBS-PRL1-2introns-cDNA-GFP. The pPCV002 binary vector was modified by introducing an *XmaI/SmaI* site on an *XbaI-BamHI* fragment from pODB8 (Louvét *et al.*, 1997). The *PRL1* promoter region extending 3.5 kb upstream of the ATG codon was PCR amplified with primers SexAI and UTR, and upon digestion used for replacement of *BstBI-XmaI* fragment of pBS-PRL1 genomic clone, to yield the construct pBS-PRL1-PROM-UTR. From the latter plasmid the promoter region extending to an *XmaI* site just upstream of the ATG codon was inserted by *XbaI-XmaI* into pPCV002-ODB to create pPCV002-PRL1-PROM-UTR. Finally, the coding region of *PRL1* fusion with the GFP gene was isolated from pBS-PRL1-2introns-cDNA-GFP and upon fill-in T4 DNA polymerase was inserted into the *SmaI* site of pPCV002-PRL1-PROM-UTR to create the *gPRL1-GFP* expression cassette in the binary vector pPCV002-PRL1-GFP.

The binary vectors pPCV812-PRL1PROM and pPCV002-PRL1-GFP carrying the *PRL1pro:GUS* and *gPRL1-GFP* reporter genes were transferred by electroporation into *Agrobacterium* GV3101 (pMP90RK) and used for transformation of WT and *prl1* mutant plants as described (Koncz and Schell, 1986). The sequences of the gene-specific primers used are listed in Table S1.

### Microscopic studies, auxin treatment, and histochemical GUS staining

Root tips of seedlings were photographed with a Leica DM750 microscope (Leica Microsystems, Wetzlar, Germany). The number (root meristem cell number is expressed as the number of cells in the cortex file extending from the QC to the transition zone) and length of cortical and mature epidermal cells were analyzed using Photoshop 8.0 (Adobe Systems Inc., San Jose, CA, USA). For auxin treatment, 6-day-old seedlings were transferred to MS medium with and without the specified concentrations of IAA (*PhytoTechnology Laboratories*<sup>®</sup>). Starch granules in the root tips were stained with an I-KI solution for 0.5 min then mounted on slides with HCG solution (chloroacetaldehyde:water:glycerol = 8:3:1) and examined immediately. DEX induction for the *35Spro:PLT2-GR* line was performed by transferring 6-day-old seedlings onto solid MS medium supplemented with 2  $\mu$ M DEX. Histochemical GUS staining was performed according to the method of Ji *et al.* (2014).

### qRT-PCR analysis

Total RNA extraction (from 300 excised root tips) and real-time PCR was performed as described as Ji *et al.* (2014). *UBQ5* (At3g62250) was used as a reference gene. The sequences of the gene-specific primers used are listed in Table S1.

### Immunolocalization assay

The PIN4 immunolocalization assay was performed using the In-situPro robot (Friml *et al.*, 2002a; Zhou *et al.*, 2010). The following antibodies and dilutions were used: anti-PIN4 (1:50) antibody and Alexa Fluor<sup>®</sup>546 secondary antibody (Molecular Probes<sup>®</sup>, A10036, Life technologies, Carlsbad, California, USA, <http://www.lifetechnologies.com/order/catalog/product/A10036>). Fluorescent samples were inspected by the Leica SP8 confocal laser scanning microscope.

### Confocal imaging and analysis

GFP fluorescence was detected with a 488 nm argon laser (25 mW, 5–10% power). Samples were scanned at a speed setting of eight using the linear mode; For PI staining, root tip samples were cut and immersed in 10  $\mu$ M PI for 1 min and then washed three times with phosphate-buffered saline, a 543 nm HeNe laser was used for image acquisition (Leica TCS SP8).

### ACKNOWLEDGEMENTS

We thank Dr. Ben Scheres (Wageningen University, Netherlands), Thomas Laux (University of Freiburg, Germany) and Klaus Palme (University of Freiburg, Germany) for sharing their published materials. This study was supported by the National Program on Key Basic Research Project (grant no. 2012CB114300) and the National Natural Science Foundation of China (grant no. 31230050 to X. L.).

### SUPPORTING INFORMATION

Additional Supporting Information may be found in the online version of this article.

**Figure S1.** Root phenotype of the *mcr1* mutant.

**Figure S2.** The *mcr1* mutation represented a new *prl1* allele.

**Figure S3.** Mitotic index in the RAM of WT and *prl1-9* seedlings.

**Figure S4.** *DR5:GUS* expression in *prl1-9* cotyledons.

**Figure S5.** *WOX5* expression is diminished in the *prl1-9* mutant.

**Figure S6.** *PLT1* and *PLT2* gene expression analysis.

**Figure S7.** *PRL1* acts independently of the *SHR/SCR* pathways.

**Table S1.** Primers used in this study.

### REFERENCES

- Aida, M., Beis, D., Heidstra, R., Willemsen, V., Bliilou, I., Galinha, C., Nussbaum, L., Noh, Y.S., Amasino, R. and Scheres, B. (2004) The PLETHORA genes mediate patterning of the Arabidopsis root stem cell niche. *Cell*, **119**, 109–120.
- Baena-González, E., Rolland, F., Thevelein, J.M. and Sheen, J. (2007) A central integrator of transcription networks in plant stress and energy signaling. *Nature*, **448**, 938–942.
- Bao, Z., Yang, H. and Hua, J. (2012) Perturbation of cell cycle regulation triggers plant immune response via activation of disease resistance genes. *Proc. Natl Acad. Sci. USA*, **110**, 2407–2412.
- Benková, E., Michniewicz, M., Sauer, M., Teichmann, T., Seifertová, D., Jürgens, G. and Friml, J. (2003) Local, efflux-dependent auxin gradients as a common module for plant organ formation. *Cell*, **115**, 591–602.
- van den Berg, C., Willemsen, V., Hage, W., Weisbeek, P. and Scheres, B. (1995) Cell fate in the Arabidopsis root meristem determined by directional signalling. *Nature*, **378**, 62–65.
- van den Berg, C., Willemsen, V., Hendriks, G., Weisbeek, P. and Scheres, B. (1997) Short-range control of cell differentiation in the Arabidopsis root meristem. *Nature*, **390**, 287–289.
- Bhalerao, R.P., Salchert, K., Bako, L., Okresz, L., Szabados, L., Muranaka, T., Machida, Y., Schell, J. and Koncz, C. (1999) Regulatory interaction of PRL1 WD protein with Arabidopsis SNF1-like protein kinases. *Proc. Natl Acad. Sci. USA*, **96**, 5322–5327.
- Bliilou, I., Xu, J., Wildwater, M., Willemsen, V., Paponov, I., Friml, J., Heidstra, R., Aida, M., Palme, K. and Scheres, B. (2005) The PIN auxin efflux facilitator network controls growth and patterning in Arabidopsis roots. *Nature*, **433**, 39–44.
- Chen, M., Liu, H., Kong, J. *et al.* (2011a) RopGEF7 regulates PLETHORA-dependent maintenance of the root stem cell niche in Arabidopsis. *Plant Cell*, **23**, 2880–2894.
- Chen, Q., Sun, J., Zhai, Q. *et al.* (2011b) The basic helix-loop-helix transcription factor MYC2 directly represses PLETHORA expression during jasmonate-mediated modulation of the root stem cell niche in Arabidopsis. *Plant Cell*, **23**, 3335–3352.
- Colon-Carmona, A., You, R., Haimovitch-Gal, T. and Doerner, P. (1999) Technical advance: spatio-temporal analysis of mitotic activity with a labile cyclin-GUS fusion protein. *Plant J.* **20**, 503–508.
- De Veylder, L., Beeckman, T., Beemster, G.T., Krols, L., Terras, F., Landrieu, I., van der Schueren, E., Maes, S., Naudts, M. and Inze, D. (2001) Functional analysis of cyclin-dependent kinase inhibitors of Arabidopsis. *Plant Cell*, **13**, 1653–1668.
- Della Rovere, F., Fattorini, L., D'Angeli, S., Velocchia, A., Falasca, G. and Altamura, M.M. (2013) Auxin and cytokinin control formation of the quiescent centre in the adventitious root apex of Arabidopsis. *Ann. Bot.* **112**, 1395–1407.
- Dello Ioio, R., Linhares, F.S., Scacchi, E., Casamitjana-Martinez, E., Heidstra, R., Costantino, P. and Sabatini, S. (2007) Cytokinins determine Arabidopsis root-meristem size by controlling cell differentiation. *Curr. Biol.* **17**, 678–682.
- Dello Ioio, R., Nakamura, K., Moubayidin, L., Perilli, S., Taniguchi, M., Morita, M.T., Aoyama, T., Costantino, P. and Sabatini, S. (2008) A genetic framework for the control of cell division and differentiation in the root meristem. *Science*, **322**, 1380–1384.
- Di Laurenzio, L., Wysocka-Diller, J., Malamy, J.E., Pysh, L., Helariutta, Y., Freshour, G., Hahn, M.G., Feldmann, K.A. and Benfey, P.N. (1996) The SCARECROW gene regulates an asymmetric cell division that is essential for generating the radial organization of the Arabidopsis root. *Cell*, **86**, 423–433.

- Ding, Z. and Friml, J. (2010) Auxin regulates distal stem cell differentiation in Arabidopsis roots. *Proc. Natl Acad. Sci. USA*, **107**, 12046–12051.
- Dinneny, J.R. and Benfey, P.N. (2008) Plant stem cell niches: standing the test of time. *Cell*, **132**, 553–557.
- Dolan, L., Janmaat, K., Willemsen, V., Linstead, P., Poethig, S., Roberts, K. and Scheres, B. (1993) Cellular organisation of the *Arabidopsis thaliana* root. *Development*, **119**, 71–84.
- Donnelly, P.M., Bonetta, D., Tsukaya, H., Dengler, R.E. and Dengler, N.G. (1999) Cell cycling and cell enlargement in developing leaves of Arabidopsis. *Development*, **215**, 407–419.
- Flores-Perez, U., Perez-Gil, J., Closa, M., Wright, L.P., Botella-Pavia, P., Phillips, M.A., Ferrer, A., Gershenzon, J. and Rodriguez-Concepcion, M. (2010) Pleiotropic regulatory locus 1 (PRL1) integrates the regulation of sugar responses with isoprenoid metabolism in Arabidopsis. *Mol. Plant*, **3**, 101–112.
- Friml, J., Benková, E., Blilou, I., Wisniewska, J., Hamann, T., Ljung, K., Woody, S., Sandberg, G., Scheres, B. and Jürgens, G. (2002a) AtPIN4 mediates sink-driven auxin gradients and root patterning in Arabidopsis. *Cell*, **108**, 661–673.
- Friml, J., Wisniewska, J., Benkova, E., Mendgen, K. and Palme, K. (2002b) Lateral relocation of auxin efflux regulator PIN3 mediates tropism in Arabidopsis. *Nature*, **415**, 806–809.
- Galinha, C., Hoffhuis, H., Luijten, M., Willemsen, V., Blilou, I., Heidstra, R. and Scheres, B. (2007) PLETHORA proteins as dose-dependent master regulators of Arabidopsis root development. *Nature*, **449**, 1053–1057.
- Grieneisen, V.A., Xu, J., Maree, A.F., Hogeweg, P. and Scheres, B. (2007) Auxin transport is sufficient to generate a maximum and gradient guiding root growth. *Nature*, **449**, 1008–1013.
- Hacham, Y., Holland, N., Butterfield, C., Ubada-Tomas, S., Bennett, M.J., Chory, J. and Savaldi-Goldstein, S. (2011) Brassinosteroid perception in the epidermis controls root meristem size. *Development*, **138**, 839–848.
- Haecker, A., Groß-Hardt, R., Geiges, B., Sarkar, A., Breuninger, H., Herrmann, M. and Laux, T. (2004) Expression dynamics of WOX genes mark cell fate decisions during early embryonic patterning in *Arabidopsis thaliana*. *Development*, **131**, 657–668.
- Helariutta, Y., Fukaki, H., Wysocka-Diller, J., Nakajima, K., Jung, J., Sena, G., Hauser, M.T. and Benfey, P.N. (2000) The SHORT-ROOT gene controls radial patterning of the Arabidopsis root through radial signaling. *Cell*, **101**, 555–567.
- de Jager, S.M., Scofield, S., Huntley, R.P., Robinson, A.S., den Boer, B.G. and Murray, J.A. (2009) Dissecting regulatory pathways of G1/S control in Arabidopsis: common and distinct targets of CYCD3;1, E2Fa and E2Fc. *Plant Mol. Biol.* **71**, 345–365.
- Ji, H., Liu, L., Li, K., Xie, Q., Wang, Z., Zhao, X. and Li, X. (2014) PEG-mediated osmotic stress induces premature differentiation of the root apical meristem and outgrowth of lateral roots in wheat. *J. Exp. Bot.* **65**, 4863–4872.
- Koncz, C. and Schell, J. (1986) The promoter of T<sub>1</sub>-DNA gene 5 controls the tissue specific expression of chimaeric genes carried by a novel type of *Agrobacterium* binary vector. *Mol. Gen. Genet.* **204**, 383–396.
- Koncz, C., Jong, F., Villacorta, N., Szakonyi, D. and Koncz, Z. (2012) The spliceosome-activating complex: molecular mechanisms underlying the function of a pleiotropic regulator. *Front. Plant Sci.* **3**, 9.
- Lee, J.H., Terzaghi, W., Gusmaroli, G., Charron, J.B., Yoon, H.J., Chen, H., He, Y.J., Xiong, Y. and Deng, X.W. (2008) Characterization of Arabidopsis and rice DWD proteins and their roles as substrate receptors for CUL4-RING E3 ubiquitin ligases. *Plant Cell*, **20**, 152–167.
- Levesque, M.P., Vernoux, T., Busch, W. et al. (2006) Whole genome analysis of the SHORT-ROOT developmental pathway in Arabidopsis. *PLoS Biol.* **4**, e249.
- Louvet, O., Doignon, F. and Crouzet, M. (1997) Stable DNA-binding yeast vector allowing high-bait expression for use in the two-hybrid system. *Biotechniques*, **23**, 816–819.
- Matsuzaki, Y., Ogawa-Ohnishi, M., Mori, A. and Matsubayashi, Y. (2010) Secreted peptide signals required for maintenance of root stem cell niche in Arabidopsis. *Science*, **329**, 1065–1067.
- Menges, M., Hennig, L., Grisse, W. and Murray, J.A. (2002) Cell cycle-regulated gene expression in Arabidopsis. *J. Biol. Chem.* **277**, 41987–42002.
- Menges, M., de Jager, S.M., Grisse, W. and Murray, J.A. (2005) Global analysis of the core cell cycle regulators of Arabidopsis identifies novel genes, reveals multiple and highly specific profiles of expression and provides a coherent model for plant cell cycle control. *Plant J.* **41**, 546–566.
- Németh, K., Salchert, K., Putnoky, P. et al. (1998) Pleiotropic control of glucose and hormone responses by PRL1, a nuclear WD protein, in Arabidopsis. *Genes Dev.* **12**, 3059–3073.
- Palma, K., Zhao, Q., Cheng, Y.T., Bi, D., Monaghan, J., Cheng, W., Zhang, Y. and Li, X. (2007) Regulation of plant innate immunity by three proteins in a complex conserved across the plant and animal kingdoms. *Genes Dev.* **21**, 1484–1493.
- Peng, Y., Ma, W., Chen, L. et al. (2013) Control of root meristem size by DA1-RELATED PROTEIN2 in Arabidopsis. *Plant Physiol.* **161**, 1542–1556.
- Pinon, V., Prasad, K., Grigg, S.P., Sanchez-Perez, G.F. and Scheres, B. (2013) Local auxin biosynthesis regulation by PLETHORA transcription factors controls phyllotaxis in Arabidopsis. *Proc. Natl Acad. Sci. USA*, **110**, 1107–1112.
- Sabatini, S., Beis, D., Wolkenfelt, H., Murfett, J., Guilfoyle, T., Malamy, J., Benfey, P., Leyser, O., Bechtold, N. and Weisbeek, P. (1999) An auxin-dependent distal organizer of pattern and polarity in the Arabidopsis root. *Cell*, **99**, 463–472.
- Sabatini, S., Heidstra, R., Wildwater, M. and Scheres, B. (2003) SCARECROW is involved in positioning the stem cell niche in the Arabidopsis root meristem. *Genes Dev.* **17**, 354–358.
- Sarkar, A.K., Luijten, M., Miyashima, S., Lenhard, M., Hashimoto, T., Nakajima, K., Scheres, B., Heidstra, R. and Laux, T. (2007) Conserved factors regulate signalling in *Arabidopsis thaliana* shoot and root stem cell organizers. *Nature*, **446**, 811–814.
- Scheres, B. (2007) Stem-cell niches: nursery rhymes across kingdoms. *Nat. Rev. Mol. Cell Biol.* **8**, 345–354.
- Segers, G., Gadisseur, I., Bergounioux, C., de Almeida Engler, J., Jacquard, A., Van Montagu, M. and Inze, D. (1996) The Arabidopsis cyclin-dependent kinase gene *cdc2bAt* is preferentially expressed during S and G2 phases of the cell cycle. *Plant J.* **10**, 601–612.
- Takatsuka, H. and Umeda, M. (2014) Hormonal control of cell division and elongation along differentiation trajectories in roots. *J. Exp. Bot.* **65**, 2633–2643.
- Tian, H., Wabnik, K., Niu, T. et al. (2014) WOX5-IAA17 feedback circuit-mediated cellular auxin response is crucial for the patterning of root stem cell niches in Arabidopsis. *Mol. Plant*, **7**, 277–289.
- Ubada-Tomas, S. and Bennett, M.J. (2010) Plant development: size matters, and it is all down to hormones. *Curr. Biol.* **20**, R511–R513.
- Ulmasov, T., Murfett, J., Hagen, G. and Guilfoyle, T.J. (1997) Aux/IAA proteins repress expression of reporter genes containing natural and highly active synthetic auxin response elements. *Plant Cell*, **9**, 1963–1971.
- Umeda, M., Umeda-Hara, C., Yamaguchi, M., Hashimoto, J. and Uchimiya, H. (1999) Differential expression of genes for cyclin-dependent protein kinases in rice plants. *Plant Physiol.* **119**, 31–40.
- Vandepoele, K., Raes, J., De Veylder, L., Rouze, P., Rombauts, S. and Inze, D. (2002) Genome-wide analysis of core cell cycle genes in Arabidopsis. *Plant Cell*, **14**, 903–916.
- Zhang, H., Han, W., De Smet, I., Talboys, P., Loya, R., Hassan, A., Rong, H., Jurgens, G., Paul Knox, J. and Wang, M.H. (2010) ABA promotes quiescence of the quiescent centre and suppresses stem cell differentiation in the Arabidopsis primary root meristem. *Plant J.* **64**, 764–774.
- Zheng, B., Chen, X. and McCormick, S. (2011) The anaphase-promoting complex is a dual integrator that regulates both MicroRNA-mediated transcriptional regulation of cyclin B1 and degradation of cyclin B1 during Arabidopsis male gametophyte development. *Plant Cell*, **23**, 1033–1046.
- Zhou, W., Wei, L., Xu, J. et al. (2010) Arabidopsis tyrosylprotein sulfotransferase acts in the auxin/PLETHORA pathway in regulating postembryonic maintenance of the root stem cell niche. *Plant Cell*, **22**, 3692–3709.
- Zuo, J., Niu, Q.W. and Chua, N.H. (2000) Technical advance: an estrogen receptor-based transactivator XVE mediates highly inducible gene expression in transgenic plants. *Plant J.* **24**, 265–273.